Article

Life rather than climate influences diversity at scales greater than 40 million years

https://doi.org/10.1038/s41586-022-04867-y

Received: 31 July 2021

Accepted: 12 May 2022

Published online: 22 June 2022

Check for updates

Andrej Spiridonov[1]✉ & Shaun Lovejoy[2]✉

The diversity of life on Earth is controlled by hierarchical processes that interact over wide ranges of timescales[1]. Here, we consider the megaclimate regime[2] at scales ≥1 million years (Myr). We focus on determining the domains of 'wandering' stochastic Earth system processes ('Court Jester'[3]) and stabilizing biotic interactions that induce diversity dependence of fluctuations in macroevolutionary rates ('Red Queen'[4]). Using state-of-the-art multiscale Haar and cross-Haar fluctuation analyses, we analysed the global genus-level Phanerozoic marine animal Paleobiology Database record of extinction rates (E), origination rates (O) and diversity (D) as well as sea water palaeotemperatures (T). Over the entire observed range from several million years to several hundred million years, we found that the fluctuations of T, E and O showed time-scaling behaviour. The megaclimate was characterized by positive scaling exponents—it is therefore apparently unstable. E and O are also scaling but with negative exponents—stable behaviour that is biotically mediated. For D, there were two regimes with a crossover at critical timescale $\Delta t_{trans} \approx 40$ Myr. For shorter timescales, D exhibited nearly the same positive scaling as the megaclimate palaeotemperatures, whereas for longer timescales it tracks the scaling of macroevolutionary rates. At scales of at least Δt_{trans} there is onset of diversity dependence of E and O, probably enabled by mixing and synchronization (globalization) of the biota by geodispersal ('Geo-Red Queen').

The nature of the macroevolution processes that dominate the formation of global biodiversity patterns has long been debated. Are these processes deterministic, equilibrial and biotically regulated[5] or are they non-equilibrial, stochastic and contingent[6,7]? The biotic regulation proposal, is often treated under the rubric 'Red Queen', a metaphor for broad-sense competition between clades[4] that provides the equilibrating force. By contrast, models emphasizing physical forcing (especially temperature) fall under the rubric 'Court Jester', after the capricious and unpredictable nature of the Earth system responsible for macroevolution[3,8]. The Earth system is highly nonlinear over wide ranges of space and timescales and, according to the latter set of 'Court Jester' hypotheses, imposes geological and climatic complexity on the biota.

Previous studies indicate diversity density dependence in macroevolution[9–13]. Macroevolution also shows typical features of nonlinear dynamics: it is highly variable and random-walk-like[6,14], a symptom of scaling with positive fluctuation exponents[15], and it shows the systematic time-dependant state shift-like changes in dominance from abiotic to biotic controlling factors[16] so that the magnitudes of (absolute) changes (shifts) are often 'spiky' or in nonlinear dynamics jargon, 'intermittent'[15].

Here, we use standard scaling methods combined with a scale-by-scale cross-correlation tool to study bounded equilibrial versus non-bounded non-equilibrial diversity dynamics[17]. How do macroevolutionary processes vary on different timescales[18]? Rosenzweig[19] pointed out that the determination of a diversity–time curve—the analogue of the diversity–area curve—is a challenge in evolutionary biogeography. Empirical and theoretical analyses suggest that different evolutionary factors and mechanistic patterns dominate at different timescales or 'tiers of time'[1,20–23].

For diversity to be regulated at global scales, regional evolutionary biotas must be coordinated. The same sets of taxa with commensurable carrying capacities should occupy space in different regions—the whole world should play by the same rules. This does not infer that diversity trajectories will be the same in all regions, just that the common nature of interactors would create qualitatively similar responses to similar disturbances. Temperature is a natural candidate for a dominant dispersive and coordinating agent; it is partially responsible for the dispersal of taxa through favourable climate conditions. At the longest timescales, plate tectonic motions should repeatedly combine formerly disjoint biotas, facilitating biotic dispersal (effective homogenization or globalization of biota). Therefore, we expect time and space scales to be linked and to play an essential role in the transition between the 'wandering' Court Jester (CJ) regime and the coordinated and constrained biotically regulated (stable) Geo-Red Queen (GRQ) regime. GRQ is understood as biotic regulation facilitated by abiotically forced dispersal. If, for example, there are two ecologically similar clades on two isolated but in all respects equivalent continents (or marine basins), a change in the climate could produce very different carrying capacities. On the other hand, if both clades are in contact, the superior one will dominate and a climate fluctuation will result in the same change in carrying capacities in both places. GRQ, by spatial mixing and matching

[1]Department of Geology and Mineralogy, Vilnius University, Vilnius, Lithuania. [2]Physics Department, McGill University, Montreal, Quebec, Canada. ✉e-mail: andrej.spiridonov@gf.vu.lt; lovejoy@physics.mcgill.ca

of clades, acts as a redundancy reducing and idiosyncratic carrying capacity equalizing force.

Fluctuations and scaling in palaeodata

The well-known limitations of palaeodata have meant that so far the debate on the scaling nature of long-term processes, such as climate, has been relatively theoretical. Over the past decade, there has been a rapid expansion and improvement in palaeodatabases. Now, what is needed is the application of powerful, yet simple to interpret data analysis techniques that permit the systematic study of processes and their interactions as functions of time (and space) scales. For example, spectral analysis is commonly used to understand the variability of macroevolutionary series[24] but the interpretation of spectral densities in climate data is often is so opaque that published spectra lack units on their abscissae. Others have shown[2] with modern instrumental and palaeoclimate data that the temperature spectrum proposed by Mitchell 1976 was in error by a factor of about a quadrillion (or 10^{15})[15]. Similarly, spectra (and other common analysis techniques) are sensitive to intermittency (the 'spikiness' of their changes) common in palaeodata. As a general consequence, the corresponding spectra show strong variability from which routine analyses would incorrectly infer deterministic cyclic processes where there were none[15].

The advance in analysis proposed by others[25] was to use the Haar wavelet to define fluctuations. For time series $T(t)$, Haar fluctuation over interval Δt is the difference between the average over the first and second halves of the interval. When average fluctuations increase with scale (Δt), they are nearly equal to the differences and when they decrease with scale they are nearly equal to anomalies (Methods). Here, we use cross-Haar analysis—the systematic determination of the correlations between fluctuations at different timescales—applying this new technique to palaeoclimate and macroevolutionary time series. This is analogous to classical cross-spectral analysis but with various advantages, including that (like the Haar fluctuations on which it is based) it is easy to apply to series with irregularly spaced measurements without the need to interpolate them to regular intervals (a practice that spuriously smoothes the statistics)[2]. Rather than estimating the correlations at fixed timescales, we estimate the unique and different root mean square (r.m.s.) fluctuation correlation coefficients, and the correlations between r.m.s. fluctuation amplitudes over a range of timescales.

Palaeoseries are typically variable over wide ranges of scales and, over any specific range, the simplest suggestion is that they are scaling, such that the fluctuations obey $\Delta F \approx \Delta t^H$, where H is the fluctuation exponent. If the series is intermittent (multifractal), as is the case for macroevolutionary time series[26], then there will be a hierarchy of exponents that describe the various statistical moments. Intermittency will be considered in future publications; here, we estimate H from the r.m.s. fluctuations. By determining changes in magnitudes of fluctuations, we estimate the scaling regimes and exponents of global macroevolutionary patterns and compare them with the scaling in megaclimate—the positive scaling climate regime[2] at timescales ≥1 Myr. By determining the correlations between Paleobiology Database Phanerozoic genus-level marine animal diversity, extinction, origination (average resolution 5.9 Myr) and megaclimate palaeotemperature time series (average resolution 1.3 Myr) as functions of timescale (Extended Data Figs. 1 and 2a), we can directly and quantitatively test the GRQ and CJ proposals as functions of scale. Second-for-third origination and extinction rates were used (Methods), as they accurately account for bin-wide gaps in the fossil record of genera[27].

The scaling patterns

The scaling of the origination (O) and extinction (E) rates show negative scaling exponents $H = -0.25$ (Fig. 1) consistent with stable, convergent dynamics (negative feedbacks) over timescales from several million

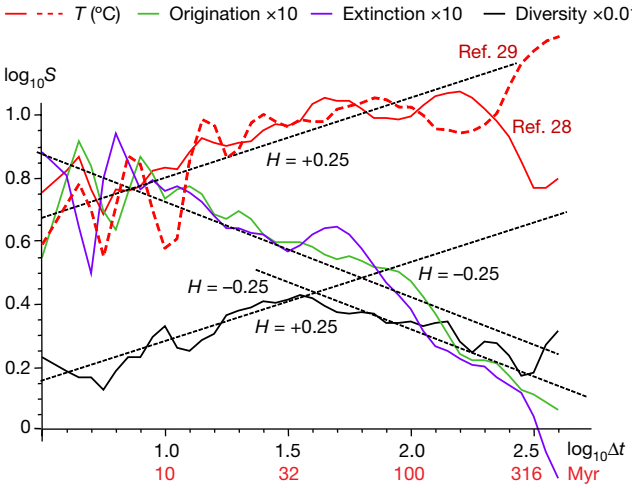

Fig. 1 | Scaling of macroevolutionary metrics and sea water palaeotemperatures. Scaling of Phanerozoic temperatures in two Phanerozoic stacks[28,29], marine animal extinction rates, origination rates and global genus diversity levels with added dashed reference lines having slopes 0.25 and −0.25. The temperatures are in °C, the extinctions and originations are second-for-third rates ×0.01 and the diversity in numbers of genera are ×0.001. Scaling in the two Phanerozoic average water temperature stacks (used in further analyses) marked as ref. [28] and ref. [29] is identical. Standard errors from macroevolutionary metric scaling curves are omitted for clarity (for average curves with uncertainties see Extended Data Fig. 3; for general issues in estimating uncertainties in scaling time series see Supplementary Information).

years to several hundred million years (Extended Data Fig. 3 gives structure functions with uncertainties). This suggests relatively quick adjustments of evolutionary rates to perturbations. The climate (palaeotemperature (T), data from refs. [28,29]) exhibits consistent positive scaling ($H = +0.25$) through the range of studied scales, with increasing variability at longer timescales. The same pattern was found in a more restricted but much more accurate dataset of Cretaceous palaeotemperatures[30] (Extended Data Fig. 2b,c). This is the signature of the apparently unstable megaclimate regime with wandering temperatures that shows no evidence of homoeostasis[2,31]. The exact values of these exponents depend on the range of scales considered; the Fig. 1, therefore, shows approximate reference lines, not regressions. However, our argument depends only on cross-correlations (below) and the signs of the exponents that determine their qualitative characters (stable versus unstable).

Neither pure E and O series nor the T climate series exhibit characteristic timescales, since their fluctuations are not confined to narrow scale ranges. By contrast, the fluctuations of biodiversity (D) have two regimes. At 'short' timescales, below about 35–40 Myr, D follows the climate scaling with $H \approx +0.25$. At longer scales, D follows the E and O scaling $H \approx -0.25$ with the global D maximal variability occurring at the crossover scale $\Delta t_{trans} \approx 40$ Myr (with fluctuations $\Delta D(\Delta t_{trans}) \approx \pm 125$ genera, $\Delta E(\Delta t_{trans}) \approx \Delta O(\Delta t_{trans}) \approx \pm 0.2$, $\Delta T(\Delta t_{trans}) \approx \pm 5$ °C (Fig. 1). If, for example, at Δt_{trans} the r.m.s. difference over a period of time Δt is 250 genera then the fluctuations at that scale are ±250/2 = 125). This suggests a transition from a wandering climate to biodynamic dominance over D fluctuations at this scale.

As the basic governing processes are scaling, the transition must be explained by interrelations between processes leading to correlations. At each scale, these can be quantified using all the available fluctuations in each series to determine the correlation coefficient at that scale by cross-Haar analysis (Fig. 2; note that the fluctuations have mean zero; Methods). With this, over the full range of timescales, D is almost exclusively negatively correlated with T (Fig. 2a). Although the

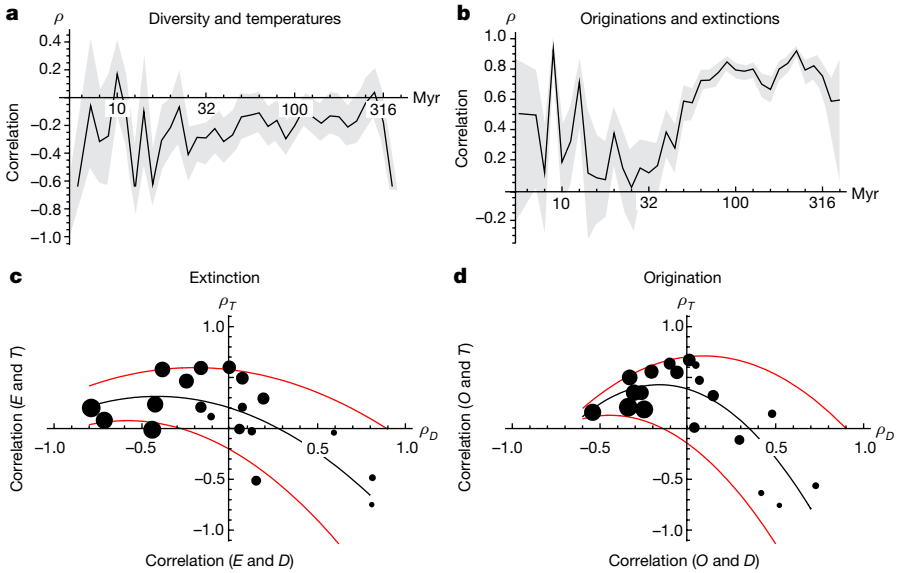

Fig. 2 | Scale-dependant correlations of macroevolutionary and palaeoclimate variables. a, Scale-dependant cross-Haar correlations of marine animal *D* with *T*. **b**, Scale-dependant cross-Haar correlations of *E* and *O* rates, with mean (black) and 1 s.d. confidence limits (transparent grey, 16–84% confidence limits). Here, the transition to a highly correlated regime starts at $\Delta t > \Delta t_{trans}$ (around 40 Myr). **c**, Cross-Haar bicorrelation plot showing the correlations of *E* rates with *D* (horizontal axis) and with *T* (vertical axis). The dots show the empirical correlation coefficients between the corresponding Haar fluctuations every factor of $10^{0.1} \approx 1.26$ in timescale, with the smallest dots indicating the shortest times and the largest dots indicating longest time scales in the range 6–300 Myr. The points in the fourth quadrant with negative temperature correlations correspond to timescales of around <15 Myr. The black line indicates the mean and the red lines are 1 s.d. confidence limits. **d**, Bicorrelation plot similar to **c** but for *O* rates with *D* and *T*. In **c** and **d**), there is a continuous transition to positive correlations of originations and extinctions with the temperatures and the transition to negative correlations with diversity as measured timescales increase. Mean, black lines; 1 s.d. confidence limits, red lines (16–84% confidence limits). All correlations are based on $n = 90$ stage-level independent data points.

correlations are weak, they are generally statistically significant. The negative correlations become weaker at longer timescales, pointing to the small effect of the longest timescale (more than Δt_{trans}) *T* fluctuations on the *D* dynamics. By contrast, we see a transition from generally low *O* and *E* correlations in the climate-dominated CJ regime (lower than (Δt_{trans})) to high correlations in the longer GRQ-dominated more than Δt_{trans} regime (Fig. 2b) with a levelling-off of correlations around $\rho = 0.8$ at timescales longer than 60 Myr. This transition from very weak to strong correlations near Δt_{trans} suggests that the transition is from globally non-equilibrial diversity dynamics (short times) to equilibrial dynamics caused by a rough balance between destructive and creative macroevolutionary mechanisms (longer timescales).

Correlations between individual fluctuations at fixed time lags/timescales, with one coefficient for each Δt can be found in Fig. 2. Figure 2c, d shows a bicorrelation diagram (for separate correlations see Extended Data Fig. 4) showing that both *O* and *E* rates experience transitions from negative correlations with *T* on shorter timescales to positive correlations at longer timescales Δt_{trans} (≈40 Myr). Figure 2c, d show that at short timescales (at most Δt_{trans}), *O* and *E* rates are only weakly negatively correlated with *T*; however, at longer timescales they become positively correlated. At increasingly longer timescales more than Δt_{trans}, *E* and *O* rates consistently become negatively correlated with the global *D* levels (Fig. 2c, d), a symptom of density dependence.

The average r.m.s. fluctuations are taken at each timescale (already an average over many fluctuations) in Fig. 3 and then their correlations are quantified over a wide range of timescales. The typical fluctuation amplitudes of temperature and diversity are compared as a function of timescales (Fig. 3a), in a graph that shows the result of the comparison of *T* and *D* r.m.s. fluctuation amplitudes. There is linear correspondence over the whole range (Pearson's correlation $\rho = 0.55$) so that *D* fluctuation amplitudes are tied to the *T* fluctuation amplitudes at all timescales. The reference line in Fig. 3a shows that for every 1 °C increase in temperature fluctuations, the diversity fluctuations increase by 23 genera.

The amplitudes of fluctuations of *E* and *O* rates with a wide scatter (independence) at short timescales are shown in Fig. 3b. The finding that fast radiation and extinction events at the global scale are essentially independent is in agreement with ref. [32]. On the other hand, at $\Delta t_{trans} \approx 40$ Myr they strongly correlate, which suggests the onset of consistent coordination between these principal macroevolutionary processes. Figure 3c, d shows that at timescales of more than Δt_{trans} there is a transition from no diversity-macroevolutionary rate correlations to strong functional correspondence.

Proximal mechanisms of scaling patterns

Negative correlations of *E* and *O* rates with *T* on shorter timescales may be because, at timescales from millions to tens of millions of years, colder conditions lead to more pronounced climate variability at (still shorter) Milankovitch timescales, which promotes allopatric speciation owing to vicariance and also extinction owing to loss of habitat (for example, Silurian and Neogene–Quaternary[33,34]). Positive correlations between extinction and origination rates with diversity levels on the shortest timescales may be explained by the effects of diversity at local and regional geographic scales as a result of insufficiency of time for global biotic mixing/coordination. Higher regional diversity pool promotes the diversity of biotically defined niches that can be filled or constructed[35]. At the same time, diverse ecosystems develop more complex networks of species trophic food webs, which could result in higher bottom-up secondary co-extinction rates[36] after extinction pulses.

At $\Delta t \geq \Delta t_{trans}$, the positive origination and extinction rate correlations with temperature (Fig. 2) may at least partially stem from the proliferation of warm climate habitats—such as biogenic reefs and carbonate environments—that are simultaneously extinction prone and diversity generating. In particular, reefs have been shown to be a notable environmental type governing global diversity in the

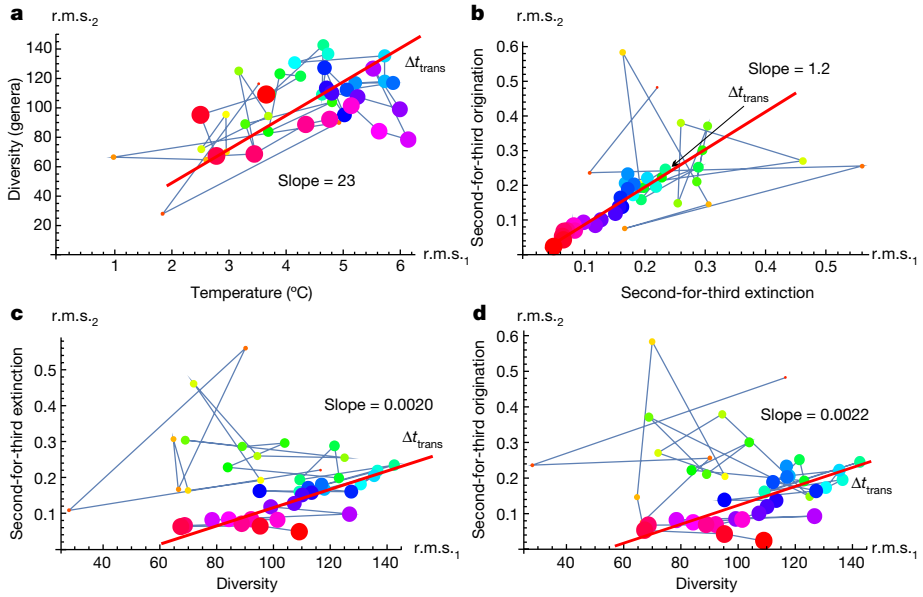

Fig. 3 | Scale-dependant correlations of macroevolutionary and palaeoclimate variables. Cross-correlations between of the average (r.m.s.) fluctuations as functions of timescale (not—as in Fig. 2—the cross-correlations between individual fluctuations at fixed timescales) are indicated by the size and colour of the points (small, short to large, long), every factor of $10^{0.1} \approx 1.26$ in timescale from smallest indicating the shortest times to largest (3.16–398.1 Myr). **a**, R.m.s. *T* changes against r.m.s. *D* changes as a function of timescale. Alignment of the cloud of points indicates that large amplitude temperature fluctuations tend to occur with large amplitude diversity fluctuations at all timescales. **b**, R.m.s. *E* against r.m.s. *O* as a function of timescales. Note the convergence of *E* and *O* magnitudes at timescales $\Delta t > \Delta t_{trans}$ (around 40 Myr) and the particularly strong correlation in the fluctuation amplitudes. **c**,**d**, R.m.s. *E* against r.m.s. *D* (**c**) and r.m.s. *O* against r.m.s. *D* (**d**). In both cases there is no direct correspondence between magnitudes of diversity and macroevolutionary rates at shorter timescales; on the other hand, at longer timescales ($\Delta t > \Delta t_{trans}$), there is a direct correspondence in magnitudes. Magnitudes of origination and extinction rates as well as diversity are synchronized after this transition timescale, which shows the presence of a crossover in macroevolution between unordered and synchronized dynamics. All fluctuation magnitudes are calculated on the basis of $n = 90$ stage-level independent data points.

Phanerozoic eon[37]. Negative temperature fluctuations created opportunities for increased global diversity at GRQ timescales. However, the absolute importance of temperature fluctuations decreased at $\Delta t > \Delta t_{trans}$.

The sizes, spatial configurations and boundaries of continents and oceanic basins work as upper-level constraints[38,39] on the regional macroevolutionary dynamics that ultimately form the global diversity pattern. Plate tectonics constantly reconfigure landmasses, which results in fission and fusion of palaeobioprovinces and directly affects opportunities for diversification due changes in provincialism, climate zonation and shelf areas. Palaeontological data demonstrate that the geodispersal—simultaneous and congruent expansion of ranges in several clades and whole regional biotas—is a crucial spatial mode of macroevolution[39] that can inhibit allopatric speciations if dispersion magnitude is very large[40]. Moreover, the long-term compositional homogenization of biota and synchronization of biotic innovations and community dynamics at the global scale is an expected first-principles outcome of clade geodispersal, facilitated by the favourable global climatic conditions, vertical tectonic movements and ultimately continental drift on the geoid. The clade geodispersal works in an irreversible ratchet-like way—biotas by dispersing in any direction on a geoid can only even out the global composition and, by doing so, even out contingent regional carrying capacities.

For extinction and origination processes to regulate diversity at a truly global scale, major continental reconfigurations, amalgamations and dispersals are needed and these start to become important at scales of tens of million years. It is, therefore, plausible that biodiversity regulation—the GRQ ($H < 0$) scaling regime for scales longer than $\Delta t_{trans} \approx 40$ Myr—is at least partially caused by tectonic processes. This explanation is also consistent with the transition from low to high correlations between extinctions and origination (Fig. 2b): their GRQ regulation of diversity involves both processes working in tandem. On timescales of tens of millions of years the main intraplate tectonic barriers could appear and disappear, the disappearance of barriers positively influencing geodispersal of clades[41]. The current plate movement rates range from approximately 0.012 to 0.18 m yr^{-1} (ref. [42]). If extrapolated to Δt_{trans}, this would result in horizontal plate movements of several hundred to several thousand kilometres.

Warm climate episodes should promote easier dispersal of taxa by eliminating thermal barriers, which are known to strongly restrict marine clades, while simultaneously decreasing provinciality of the biosphere[43]. Many warming episodes were associated with important clade dispersal events and increases in cosmopolitanism[44,45]. The geometry of the planet and its latitudinal patterns of insolation determine the topology of climatic zones, where warm areas are directly connected to single latitudinal belts and cool areas are restricted to the two disjoint regions around geographic poles. This topological feature restricts the effectiveness of the dispersal of cold-adapted clades by expansion of cold climate bands. Only the most extreme cooling events, such as the end-Ordovician Ice Age[46], would be sufficient to cool down the equatorial zone enough for trans-hemispheric dispersal and outstanding global increase in cosmopolitanism.

Warm climate impulses promote dispersal on all considered timescales and, if this warm regime is sustained long enough for plate tectonics to transfer biotas to other regions, this will have maximal effect for global scale dispersal through latitudes as well as longitudes. The dispersal of generalist taxa will inhibit local differentiation of biotas by competition and especially predation that changes and ultimately converges the food web structure[47,48].

The confidence intervals around the scale-specific correlations (Fig. 2 and Extended Data Fig. 4; Supplementary Information) may be large. At least four factors are responsible: (1) accuracy of the reconstructed

climate states from proxies and macroevolutionary variables derived from the occurrence data (these constantly improve with time); (2) the wide range of variability in Earth system at all scales (the Phanerozoic eon may not be sufficiently long for accurate representation of variability at all studied timescales); (3) internal and unaccounted complexity of macroevolutionary dynamics; (4) the fact that for many lags there may be only a few intervals that have enough disjoint fluctuations to justify an estimate of the correlations (particularly true for longer timescales).

It is possible that two regimes of diversity scaling can track a globally important geophysical variable that can structure both—the fossil record and the diversity estimated from it (CJ rules at all scales). In this case, diversity and an environmental proxy variable should exhibit similar scaling patterns. An obvious possibility is sea level or oceanic crustal production rates (as a proxy for tectonism). We tested their scaling using Haar fluctuations (Extended Data Fig. 5). Both these variables (as well as megaclimate) show $H > 0$ scaling behaviour up to at least 100 Myr with no sign of stabilization near Δt_{trans} of biodiversity dynamics (Fig. 1 and Extended Data Fig. 5). Sea level has a high H of around +0.7 up to 100 Myr (2.5× longer than Δt_{trans}), after which it flattens out at high variability levels on the longest timescales. Sea floor production shows a similarly steep strongly wandering regime H of around +0.5. Moreover, if any such mechanisms of externally forced biodiversity exist, it would be difficult to explain why there is negative diversity dependence of extinction and origination rates on the longest timescales. The same high diversity levels, for example, could be sustained by close balance of high macroevolutionary rates, which is not observed empirically. This again points to the importance of negative feedbacks on long timescales by diversity on global originations and extinctions. Negative scaling of macroevolutionary rates and also a monotonic trend toward negative correlations between rates and diversity with timescale is prima facie evidence for biotic regulation on longer and longer timescales.

Our conceptual model, which integrates all described patterns, states that $H > 0$ scaling destabilizing climate competes with $H < 0$ density dependence of macroevolutionary rates for control of global diversity (Fig. 4a). As a result of long-term biotic homogenization, caused by warm climate fluctuations and tectonic movement, density dependence starts to prevail and biota become effectively global. This competition of factors results in crossover between two scaling regimes: wandering global D behaviour at $\Delta t < \Delta t_{trans}$ (CJ) and biotically constrained stabilizing behaviour at $\Delta t > \Delta t_{trans}$ (GRQ) (Fig. 4b). Do biota ever become effectively global? The answer appears to be no, because innovations and extinctions destroy spatial similarity gains at a global scale by previous homogenizations. However, for long timescales, the answer is yes, because unsteady tectonics and wandering climate effectively mix locally produced innovations and even out large heterogeneities.

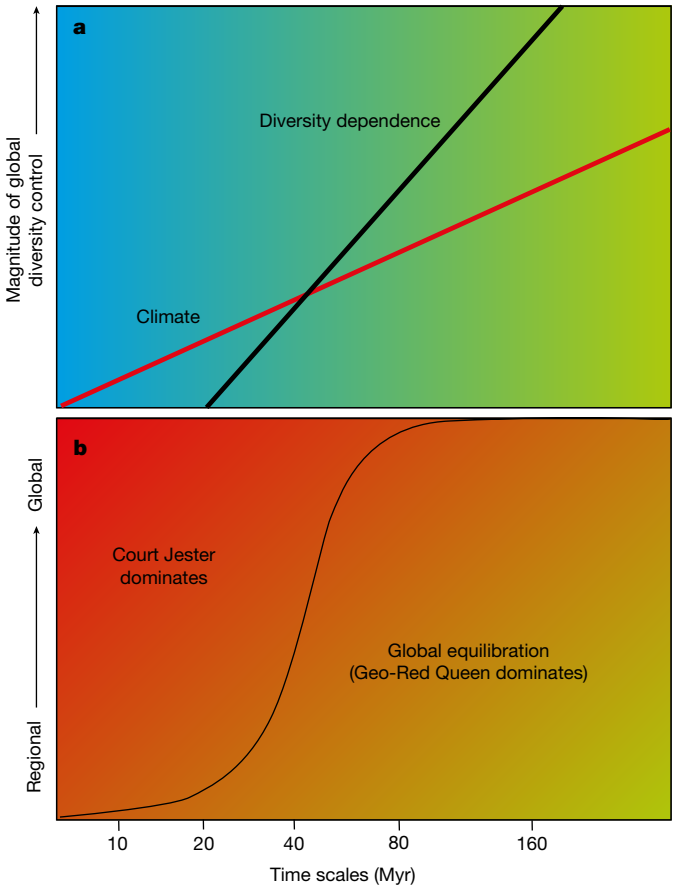

Fig. 4 | Space–time scaling of dominance in macroevolutionary modes. **a**, Conceptual diagram showing relative influence of the climate and diversity dependence on the global diversity as a function of timescales. **b**, Conceptual diagram showing space–time dominions of divergent non-equilibrial dynamics (CJ) and geodispersal-mediated diversity equilibration (GRQ).

Conclusions

Our main finding was clear qualitative change in diversity behaviour (scaling break) at $\Delta t_{trans} \approx 40$ Myr. Whereas at short timer scales, diversity dynamics follows temperature (CJ), at longer timescales, it follows extinction–origination (GRQ) scaling. The existence of corresponding causal links was further supported by studies of fluctuation cross-correlations at each scale: for $\Delta t > \Delta t_{trans}$ not only do origination and extinction rates become highly correlated with each other but their magnitudes become similar and they start to strongly negatively correlate with standing diversity levels.

These patterns show that Gaia-like self-regulating mechanisms of biota and temperature are unlikely to operate as neither T nor D shows stabilization at shorter macroevolutionary timescales. At the longer timescales, megaclimate wanders further and temperature fluctuations achieve larger and larger fluctuation amplitudes, while diversity converges to long-term average values. This implies that, at timescales between 40 and 500 Myr, diversity becomes increasingly insensitive to wide swings in climatic states.

These patterns suggest an important role for spatial processes in forming qualitatively distinct regimes of biodiversity dynamics described by different emergent scaling laws. Further studies, using regionally localized fossil and climate state data, should throw light on the emergence of long-term equilibrial biodiversity dynamics. Our explanation of crossover between high-frequency wandering and low-frequency stabilizing regimes predicts that at smaller (for example, continental) spatial scales, this transition should appear at shorter timescales. The crossover scale at global level should also be shorter when the rate of tectonic movement is faster or intrinsic geodispersal rates of separate clades are higher. As scaling multifractal cascade processes are typified by hierarchy of sharply differing states with varying durations[26,49,50], the intermittency—an issue of sudden changes in macroevolutionary states—needs separate attention. The results of our study, suggest that a high Cenozoic marine diversity level is probably a transient multidecamillion-year scale feature related to cold megaclimate fluctuation, which should decay as time passes.

Online content

Any methods, additional references, Nature Research reporting summaries, source data, extended data, supplementary information, acknowledgements, peer review information; details of author contributions and competing interests; and statements of data and code availability are available at https://doi.org/10.1038/s41586-022-04867-y.

1. Gould, S. J. *The Structure of Evolutionary Theory* (Harvard Univ. Press, 2002).
2. Lovejoy, S. A voyage through scales, a missing quadrillion and why the climate is not what you expect. *Clim. Dynam.* **44**, 3187–3210 (2015).
3. Barnosky, A. D. Distinguishing the effects of the Red Queen and Court Jester on Miocene mammal evolution in the northern Rocky Mountains. *J. Vertebr. Paleontol.* **21**, 172–185 (2001).
4. Van Valen, L. A new evolutionary law. *Evol. Theory* **1**, 1–30 (1973).
5. Sepkoski, J. J. J. in *Evolutionary Paleobiology* (eds Jablonski, D. et al.) 211–255 (Univ. of Chicago Press, 1996).
6. Cornette, J. L. & Lieberman, B. S. Random walks in the history of life. *Proc. Natl Acad. Sci. USA* **101**, 187–191 (2004).
7. Hoffman, A. in *Neutral Models in Biology* (eds Nitecki, M. H. & Hoffman, A.)133–146 (Oxford Univ. Press, 1987).
8. Benton, M. J. The Red Queen and the Court Jester: species diversity and the role of biotic and abiotic factors through time. *Science* **323**, 728–732 (2009).
9. Alroy, J. The shifting balance of diversity among major marine animal groups. *Science* **329**, 1191–1194 (2010).
10. Alroy, J. Geographical, environmental and intrinsic biotic controls on Phanerozoic marine diversification. *Palaeontology* **53**, 1211–1235 (2010).
11. Close, R. A. et al. The apparent exponential radiation of Phanerozoic land vertebrates is an artefact of spatial sampling biases. *Proc. R. Soc. B* **287**, 20200372 (2020).
12. Foote, M. in *Evolution after Darwin: The first 150 years* (eds Bell, M. A. et al.) 479–510 (Sinauer Associates, 2010).
13. Foote, M., Cooper, R. A., Crampton, J. S. & Sadler, P. M. Diversity-dependent evolutionary rates in early Palaeozoic zooplankton. *Proc. R. Soc. B* **285**, 20180122 (2018).
14. Alroy, J. et al. Phanerozoic trends in the global diversity of marine invertebrates. *Science* **321**, 97–100 (2008).
15. Lovejoy, S. Spectra, intermittency, and extremes of weather, macroweather and climate. *Sci. Rep.* **8**, 12697 (2018).
16. Eichenseer, K. et al. Jurassic shift from abiotic to biotic control on marine ecological success. *Nat. Geosci.* **12**, 638–642 (2019).
17. Patzkowsky, M. E. Origin and evolution of regional biotas: a deep-time perspective. *Annu. Rev. Earth Planet. Sci.* **45**, 471–495 (2017).
18. Jablonski, D. Approaches to macroevolution: 2. Sorting of variation, some overarching issues, and general conclusions. *Evol. Biol.* **44**, 451–475 (2017).
19. Rosenzweig, M. L. *Species Diversity in Space and Time* (Cambridge Univ Press, 1995).
20. Gould, S. J. The paradox of the first tier: an agenda for paleobiology. *Paleobiology* **11**, 2–12 (1985).
21. Erwin, D. H. in *Chance in Evolution* (eds Ramsey, G. & and Pence, C. H.) 279–298 (Univ. Chicago Press, 2016).
22. Jablonski, D. Scale and hierarchy in macroevolution. *Palaeontology* **50**, 87–109 (2007).
23. Jablonski, D. Approaches to macroevolution: 1. General concepts and origin of variation. *Evol. Biol.* **44**, 427–450 (2017).
24. Newman, M. & Palmer, R. *Modeling Extinction* (Oxford Univ. Press, 2003).
25. Lovejoy, S. & Schertzer, D. Haar wavelets, fluctuations and structure functions: convenient choices for geophysics. *Nonlin. Processes Geophys.* **19**, 513–527 (2012).
26. Plotnick, R. E. & Sepkoski, J. J. J. A multiplicative multifractal model of originations and extinctions. *Paleobiology* **27**, 126–139 (2001).
27. Alroy, J. A more precise speciation and extinction rate estimator. *Paleobiology* **41**, 633–639 (2015).
28. Song, H., Wignall, P. B., Song, H., Dai, X. & Chu, D. Seawater temperature and dissolved oxygen over the past 500 million years. *J. Earth Sci.* **30**, 236–243 (2019).
29. Veizer, J. et al. $^{87}Sr/^{86}Sr$, $\delta^{13}C$ and $\delta^{18}O$ evolution of Phanerozoic seawater. *Chem. Geol.* **161**, 59–88 (1999).
30. O'Brien, C. L. et al. Cretaceous sea-surface temperature evolution: constraints from TEX86 and planktonic foraminiferal oxygen isotopes. *Earth Sci. Rev.* **172**, 224–247 (2017).
31. Lovejoy, S. *Weather, Macroweather, and the Climate: Our Random Yet Predictable Atmosphere* (Oxford Univ. Press, 2019).
32. Cuthill, J. F. H., Guttenberg, N. & Budd, G. E. Impacts of speciation and extinction measured by an evolutionary decay clock. *Nature* **588**, 636–641 (2020).
33. Crampton, J. S., Cooper, R. A., Sadler, P. M. & Foote, M. Greenhouse–icehouse transition in the Late Ordovician marks a step change in extinction regime in the marine plankton. *Proc. Natl Acad. Sci. USA* **113**, 1498–1503 (2016).
34. Van Dam, J. A. et al. Long-period astronomical forcing of mammal turnover. *Nature* **443**, 687–691 (2006).
35. Erwin, D. H. Seeds of diversity. *Science* **308**, 1752–1753 (2005).
36. Roopnarine, P. D. Extinction cascades and catastrophe in ancient food webs. *Paleobiology* **32**, 1–19 (2006).
37. Close, R. A., Benson, R. B. J., Saupe, E. E., Clapham, M. E. & Butler, R. J. The spatial structure of Phanerozoic marine animal diversity. *Science* **368**, 420–424 (2020).
38. Eldredge, N. *Unfinished Synthesis: Biological Hierarchies and Modern Evolutionary Thought* (Oxford Univ. Press, 1985).
39. Lieberman, B. S., MillerIII, W. & Eldredge, N. Paleontological patterns, macroecological dynamics and the evolutionary process. *Evol. Biol.* **34**, 28–48 (2007).
40. Stigall, A. L. Invasive species and biodiversity crises: testing the link in the Late Devonian. *PLoS ONE* **5**, e15584 (2010).
41. Lam, A. R., Stigall, A. L. & Matzke, N. J. Dispersal in the Ordovician: speciation patterns and paleobiogeographic analyses of brachiopods and trilobites. *Palaeogeogr. Palaeoclimatol. Palaeoecol.* **489**, 147–165 (2018).
42. DeMets, C., Gordon, R. G., Argus, D. F. & Stein, S. Current plate motions. *Geophys. J. Int.* **101**, 425–478 (1990).
43. Valentine, J. W., Foin, T. C. & Peart, D. A provincial model of Phanerozoic marine diversity. *Paleobiology* **4**, 55–66 (1978).
44. Button, D. J., Lloyd, G. T., Ezcurra, M. D. & Butler, R. J. Mass extinctions drove increased global faunal cosmopolitanism on the supercontinent Pangaea. *Nat. Commun.* **8**, 733 (2017).
45. Spiridonov, A. et al. Integrated record of Ludlow (Upper Silurian) oceanic geobioevents—coordination of changes in conodont, and brachiopod faunas, and stable isotopes. *Gondwana Res.* **51**, 272–288 (2017).
46. Sheehan, P. & Coorough, P. Brachiopod zoogeography across the Ordovician–Silurian extinction event. *Geol. Soc. Lond. Mem.* **12**, 181–187 (1990).
47. Borrelli, J. J. et al. Selection on stability across ecological scales. *Trends Ecol. Evol.* **30**, 417–425 (2015).
48. Stanley, S. M. Predation defeats competition on the seafloor. *Paleobiology* **34**, 1–21 (2008).
49. Spiridonov, A., Brazauskas, A. & Radzevičius, S. Dynamics of abundance of the mid- to late Pridoli conodonts from the eastern part of the Silurian Baltic Basin: multifractals, state shifts, and oscillations. *Am. J. Sci.* **316**, 363–400 (2016).
50. Lovejoy, S. & Schertzer, D. *The Weather and Climate: Emergent Laws and Multifractal Cascades* (Cambridge Univ. Press, 2013).

Methods

Paleobiology Database and macroevolutionary metrics

Previous studies have attempted to investigate functional relations between taxonomic diversity and the dynamics of key environmental/geophysical variables[51,52]. Some studies focused on the finest scale dynamics[53] of fluctuations (millions to tens of millions of years), some explored the effects of hierarchical interactions of long and short fluctuations on extinction and origination[54,55] and others aimed to recover hierarchical spectral and cross-spectral interactions of possible Earth system and diversity cycles[56]. Here, we use a set of marine animal biodiversity and key palaeoenvironmental variables (mostly mean ocean palaeotemperatures) to show their scale-by-scale fluctuation distributions, their scaling functions and their cross-interactions, and to identify important factors driving the divergence and stability of the marine biosphere.

The taxonomic occurrence data were downloaded on 5 June 2019 from the Paleobiology Database (https://paleobiodb.org/). The specified time range of analysed taxa was set between 545 and 0 Myr and included all animal genera found in the marine sediments, excluding uncertain genera and including only regular taxa (no ichnotaxa). The dataset included 765,125 occurrence records.

Species level is preferred for macroevolutionary analysis but at the global scale (even in the best-known taxa with good fossilization and detection potential[57]) the fossil record is incomplete at this level. Variability of conditions of preservation results in variable recognition potential making it impossible to assign specimens to the species level but assignment to higher taxa is still possible. This means that larger absolute number of occurrences could be used for numerical estimation of macroevolutionary metrics. We performed our analysis at the genus level, because it is the level of taxonomic hierarchy closest to the species level and has higher temporal and spatial completeness.

Variations in genus diversity (richness) and extinction and origination rates, owing to constraints of a hierarchical genealogical structure, should represent lower-level species dynamics better that higher levels such as family- or order-level data, because the variations in parameters are less damped by taxonomic coarsening[58]. Taxonomic simulations found that finely clumped phylogenetic trees (including paraphyletic) accurately show lower-level origination and extinction processes[59]. It could be argued that genera from different phyla could represent qualitatively different biological groupings. But the same argument could be given for species (or any other taxonomic level), because species also vary widely in their internal structure, sometimes forming so-called ephemeral species (their presence is suggested on empirical grounds in the fossil record[60]), which can branch and be later reabsorbed into the parent lineage. As this taxonomic definitional inhomogeneity is not notably biased through geological time, this is of little concern for our study. Empirically, if there is enough taxonomic information on a global scale (and even if the exact placements of taxa change with time as taxonomy advances and there is constant revision of their temporal distributions), the basic quantitative patterns of macroevolution can still be distilled[61]. If genus-level data are abundant and sampling standardization protocols implemented, the macroevolutionary patterns produced are close to the species-level patterns[62].

Global biodiversity and macroevolutionary rates were calculated using divDyn package implemented in the R computational environment[63,64]. The stratigraphic subdivisions of Cambrian and Ordovician periods were augmented for higher accuracy using scripts available in the divDyn vignette description[65,66]. For calculation of macroevolutionary metrics we used Paleobiology Database time bins, which started at 525 Myr and ended at 1.3 Myr and had average duration of 5.9 Myr. The unbinned data (such as ref. [67]) are the best way to quantify diversity. Binning could pose a significant problem when the durations of genera are shorter than duration of stages, producing spurious white noise-like behaviour (with exponent $H = -1/2$). But this is not the case with the Phanerozoic marine animal dataset analysed here. The average duration of Phanerozoic marine invertebrate species is about 11 Myr (genera 28.4 Myr)[68], much longer than average duration of stages (bins) used in the analysis. No palaeobiological proxy analysed here exhibits white noise regime.

To standardize the sampling rate, we used SQS subsampling routine in divDyn, with shareholder quorum $q = 0.7$. Diversity is shown to be robust to a wide range of choices in this parameter[10]. Number of genera per Paleobiology Database stage was used as a measure of diversity or genus richness. The origination (p) and extinction (q) per capita rates (proportions) were also calculated in the divDyn package, using the second-for-third algorithmic iterative approach that accounts for the effects of gaps in the fossil ranges of taxa[27,64]. Per capita rates of origination and extinction are a natural measure, as the change is genealogical and depends on the reproduction (branching) or termination of separate lineages; absolute numbers (diversity) will vary with exponential rates[69]. Absolute measures could also be used when the absolute numbers of species are large enough for the problem at hand, for example, in comparing the absolute influence of biota on biogeochemical processes. This could be justified if each taxon contributes a comparable magnitude of influence to the environment (for example, in sequestration of carbon). As here we are concerned with the shapes of diversity curves at all available timescales and processes that are important at the lowest available taxonomic level (genus level), some version of per capita rates should be used in the analysis. The extinction and origination rates were not normalized for the durations of operational PaleoDB stages, because most of the evolutionary turnover is near-instantaneous (pulsed) at the scale of stratigraphic stages[70,71]. All macroevolutionary metric averages and their standard deviations were calculated by averaging 100 Monte Carlo subsamplings performed on the downloaded dataset. The average values were used for the analysis. The whole set of subsamplings was used for the estimation of confidence intervals in scaling relations. Diversity, extinction and origination values were assigned to the middles of stratigraphic intervals.

Palaeotemperature data

As a temperature proxy we used one of the latest stacks of the sea surface temperatures that spans the past 498 Myr (ref. [28]), from the Late Cambrian to the Quaternary periods. The average resolution of averaged global sea surface temperature stack is about 1.3 Myr, with median time resolution being 1 Myr. The stack is based on the compilation of water palaeotemperature estimates based on the δ^{18}O record of diagenetically unaltered phosphatic fossils (for the Palaeozoic era) and carbonatic and phosphatic fossils for the Mesozoic and Cenozoic eras. The temperatures used were calculated assuming constant δ^{18}O average composition of global water[28]. A similar stack by others[29] was used in the construction of Fig. 1 (Extended Data Fig. 2a) to test the robustness of scaling. In all further analyses newer and more evenly covered in time the stack by ref. [28] stack was used. The data are available as supplementary material to the cited articles[28,29].

Estimating of palaeotemperatures from δ^{18}O is a complex procedure, especially at the longest timescales. The estimation of early Palaeozoic era temperatures is confounded by possible inconstancy of isotopic composition of average oceanic water and more pronounced diagenesis than sediments of the earlier eras[72]. The consistency of conodont apatite δ^{18}O measurements with the bulk and clumped isotopes in carbonate rocks and also with other more qualitative indicators show probable climatic origin of the variability during the Cambrian to early Ordovician periods, where diagenesis-induced stable oxygen isotopic variability was of secondary importance[73]. The δ^{18}O measurements of foraminifera are a major source of Mesozoic–Cenozoic palaeoclimate data, although this source could be strongly affected by burial history and diagenesis[74]. Therefore, we tested the robustness of scaling of the Phanerozoic-scale sea water palaeotemperature trends by analysing compilations of Cretaceous

sea surface temperatures estimated from pristinely preserved planktonic foraminifera and archaean lipid-based TEX_{86} index, independently analysing trends in high (>±48°) and low (<±30°) palaeolatitudes[30]. Over the overlapping range of timescales, the $\delta^{18}O$ scalings (Extended Data Fig. 2b,c) are essentially identical to the patterns found using the lower resolution but much longer stacks (ref. [29] and ref. [28]) that had more heterogenous sources (Fig. 1). Despite differences in quality and the sources of information on the palaeotemperatures in different parts of the palaeorecords, the scaling is quantitatively consistent, indeed the scaling exponent is nearly the same ($H \approx +0.25$).

The exact physical interpretation of the climate proxy is not too important. As long as the proxy is strongly physically related to (and correlated with) temperature, the latter will also probably be scaling, although not necessarily with the same exponent. The reason is that scaling is a symmetry so that, if it is broken by a strongly interacting dynamical process that operates only over a narrow range of scales, any related interacting processes with their palaeo-indicators will also have broken symmetries. Conversely, the absence of a strong scale break in one series is positive evidence that there is not a break in other series produced by strongly interacting processes.

Tectonic and sea level proxies

Palaeotemperature, though frequently noisy, is probably one of the most reliable and densely covered geophysical proxies of environmental forcing of the biota. As further geophysical proxies, sea level and the production of sea floor were studied for their scaling characteristics (Extended Data Fig. 5). Often sea level studies use $\delta^{18}O$ as a proxy for sea level, especially in unravelling the effects of glacioeustasy[75]. Since we used the $\delta^{18}O$ record as a proxy of palaeotemperatures, in order to avoid redundancy in proxies, we used strontium isotopic ($^{87}Sr/^{86}Sr$) variability-based reconstruction[76] here as a proxy of sea level. The sea level proxy record spans the Phanerozoic eon and the Neoproterozoic era (past 837 Myr). The resolution of this record is 1 Myr (837 sea level estimates). As the proxy of global tectonic activity we used the production rate of the sea floor[77], which is proportional to the total mid-ocean ridge length and its product with average spreading rate. The record of sea floor production spans the past 231 Myr with a resolution of 1 Myr (231 estimates).

Haar fluctuations

The traditional technique for analysing times series as functions of scale uses Fourier spectra but these have problems of interpretation[2] and are prone to spurious periodicity estimation[15]. In addition, although cross-spectra can be used for studying statistical relations between specific frequencies, they require ensembles of series and are ill-adapted for single realizations (as here, from unique planet Earth).

In palaeontological time series analyses, data are often detrended and differenced, yielding fluctuations at the smallest scale that is later used in the statistical analyses (example studies are refs. [49,78,79]). This differencing approach to the analysis of time series is a type of wavelet (the 'poor man's' wavelet) that can be used for the whole range of scales. However, it is valid only when scaling coefficient $H \in (0;1)$ (ref. [50]).

Fortunately, a convenient technique that is both easy to apply and to interpret exists: Haar fluctuations[25] valid for $-1 < H < 1$ (both for differences and anomalies). No detrending is needed or even advised (except where the presence of trend is known beforehand, for example, diurnal cycle in weather) for the implementation of this technique, because a trend is treated as an ordinary largest scale fluctuation. Subtraction of a trend could lead to a distortion of a scaling pattern.

For a time series $T(t)$ (for example, palaeotemperature), the Haar fluctuation $\Delta T(\Delta t)$ at timescale Δt is:

$$\Delta T(\Delta t)_{\mathrm{Haar}} = \frac{2}{\Delta t}\int_{t-\Delta t/2}^{t} T(s)\mathrm{d}s - \frac{2}{\Delta t}\int_{t-\Delta t}^{t_0+\Delta t/2} T(s)\mathrm{d}s$$

that is, the Haar fluctuation (based on the first wavelet[80]) at timescale Δt, is the difference between the average of the first and second halves of interval Δt. Figures 1–3 are based on all the Haar fluctuations over all the disjoint intervals in their respective time series. The qth-order structure function is defined by:

$$\langle |\Delta T|^{q}_{\mathrm{Haar}} \rangle \propto \Delta t^{\xi(q)}$$

The angle brackets are averages over all the fluctuations in the series and over all the series (if there is more than one). Figure 1 uses the r.m.s. fluctuation at that scale, the square root of the average over the squares, with exponent $\xi(2)/2$. The basic fluctuation exponent H is defined with respect to the mean fluctuation:

$$\langle |\Delta T|_{\mathrm{Haar}} \rangle \propto \Delta t^{H}$$

so that $H = \xi(1)$. In general, for scaling processes (over scaling regimes), $T(t)$ is intermittent, multifractal with concave $\xi(q)$ often characterized by the intermittency exponent $C_1 = H - \xi'(1)$. In the (non-intermittent, quasi-Gaussian) approximation used here, $\xi(q) = Hq$ so that $C_1 \approx 0$ and $\xi(2)/2 = H$ (see ref. [25] for a review). We only use the second ($q = 2$) moment because it is conventional and is trivially related to the spectral exponent.

Figure 1 also multiplies the raw Haar fluctuations by the canonical calibration factor 2 so that the Haar fluctuations are close to the more usual fluctuations: that is, either differences or anomaly fluctuations. Recall that the difference and anomaly fluctuations at scale Δt are:

$$\Delta T(\Delta t)_{\mathrm{diff}} = T(t) - T(t-\Delta t)$$

$$\Delta T(\Delta t)_{\mathrm{anom}} = \frac{1}{\Delta t}\int_{t-\Delta t}^{t} T'(s)\mathrm{d}s; \quad T'(t) = T(t) - \overline{T}$$

where $\overline{T}$ is the mean of $T(t)$ over the entire series. With the factor 2 calibration, typical (average) ΔT_{Haar} is related to ΔT_{diff} and ΔT_{anom} as:

$$\Delta T_{\mathrm{Haar}} \approx \begin{array}{ll} \Delta T_{\mathrm{dif}}; & 0 < H < 1 \\ \Delta T_{\mathrm{anom}}; & -1 < H < 0 \end{array}$$

This means that when the slope in Fig. 1 is positive, the fluctuations can be interpreted as typical changes over Δt; and when it decreases with scale, they can be interpreted as typical anomalies over scale Δt. Also, if we interpret the r.m.s. fluctuations in terms of typical fluctuations ΔF about a mean, then the typical fluctuations are $\Delta F(\Delta t) \approx \pm\frac{1}{2}\langle \Delta F(\Delta t)^2 \rangle^{1/2}$. This approximation is indicated in the section 'The scaling patterns'.

At longer and longer times, there are fewer and fewer disjoint intervals. When we reach intervals half the length (here about 250 Myr), there are two disjoint intervals. At longer timescales, the algorithm still uses two intervals: one that starts at the beginning and the other that ends at the end. For example, at the longest scales considered (close to 400 Mys), one fluctuation is estimated over the range 1–400 Myr and the other from about 100 Myr to about 500 Myr. Although they overlap noticeably, they still contain information about the variability at these scales.

The intermittency (sudden spikes) can strongly influence analysis, although in our case, as shown by fitting to cumulative distributions of absolute magnitudes of fluctuations[15], the power law exponent q_D values in all time series are more than 2, which indicates that lower order moments (mean and variance), which were used in the analysis, should converge. More precisely, analysis shows that estimates of the second-order moment do not spuriously depend on the single largest value in the sample. Indeed, our results would not be qualitatively changed if they had been based only on the mean ($q = 1$ moment) that is more robust (less sensitive to extremes).

The accuracy of the data and the amount of noise in them directly influence the final result in any technique. We tested this possible sensitivity of the analysis by comparing and incorporating two different palaeoclimate records[28,29] separated by two decades of research and based on different timescale calibrations. As can be seen from Extended Data Fig. 2, although both records are characterized by similar general shapes, at first glance they seem different. Although the stack by ref. [29] has higher resolution, it has many large gaps. The stack by ref. [28] is more homogeneous (at about 1 Myr timescale) although it may be missing some large-magnitude extremes (for example, related to Permian–Triassic extinction event). Despite these differences, patterns of scaling in both stacks are essentially identical (Fig. 1), demonstrating the robustness of the method used and of the data at hand.

Cross-Haar fluctuation correlations

Beyond ease of calculation and interpretation, a further advantage of using Haar fluctuations (when compared, for example, to cross-spectral analysis) is that it is easy to quantify the correlations between two series as a function of timescale (Figs. 2 and 3). This can be done in two ways: correlations of separate fluctuations and correlations between typical amplitudes as functions of time scale. We limited the application to the lag = 0 case, because the limited lengths of time series would have restricted the analysis of longest timescales.

Consider two time series, $A(t)$ and $B(t)$. Let $\Delta A(\Delta t)$ and $\Delta B(\Delta t)$ indicates the (Haar) fluctuations of A and B (with overall mean removed so that $\langle \Delta A \rangle = \langle \Delta B \rangle = 0$) at time Δt:

$$\langle \Delta A^2(\Delta t) \rangle = \frac{1}{N(\Delta t)} \sum_{i=1}^{N(\Delta t)} \Delta A_i(\Delta t)^2$$

The angle brackets are averages over all the ($N(\Delta t)$, disjoint) fluctuations at scale Δt (if more than one series was available, they would be included in the average). The (normalized) fluctuation correlation coefficients are given by:

$$\rho_{\Delta A, \Delta B}(\Delta t) = \frac{\langle \Delta A^2 \rangle + \langle \Delta B^2 \rangle - \langle (\Delta (A - B))^2 \rangle}{2 \langle \Delta A^2 \rangle^{1/2} \langle \Delta B^2 \rangle^{1/2}}$$

(the numerator is $2\Delta A \Delta B$: using the above formula, correlations can be calculated from the Haar fluctuations of A, B, $(A - B)$). These were used in Fig. 2.

Rather than determining the correlations at each timescale, we can (Fig. 3) estimate the cross-amplitude correlations over a wide range of timescales:

$$\rho_{\langle \Delta A^2 \rangle^{1/2}, \langle \Delta B^2 \rangle^{1/2}} = \frac{\overline{(\langle \Delta A^2 \rangle \langle \Delta B^2 \rangle)^{1/2}} - \overline{\langle \Delta A^2 \rangle^{1/2}}\ \overline{\langle \Delta B^2 \rangle^{1/2}}}{\sigma_{\langle \Delta A^2 \rangle^{1/2}} \sigma_{\langle \Delta B^2 \rangle^{1/2}}};$$

$$\sigma^2_{\langle \Delta A^2 \rangle^{1/2}} = \overline{(\langle \Delta A^2 \rangle)} - (\overline{\langle \Delta A^2 \rangle^{1/2}})^2$$

$$\sigma^2_{\langle \Delta B^2 \rangle^{1/2}} = \overline{(\langle \Delta B^2 \rangle)} - (\overline{\langle \Delta B^2 \rangle^{1/2}})^2$$

The overbars are averages over all timescales.

The estimation of cross-amplitude correlations between studied variables provides further information about the balance of factors that creates macroevolutionary patterns. Even if origination and extinction rates are highly correlated at a given scale, the resulting diversity pattern could be unbalanced if average amplitudes of these rates at given timescales are different. For example, if extinction amplitude is systematically higher than average origination magnitude, the resulting dynamics will result in systematic average drops in diversity at a given timescale. If cross-amplitudes between extinction and origination relations drift unpredictably as a function of scale, this indicates non-coordination and nonlinearity between these two variables. On the other hand, a functional relation that is close to the identity line, means that the fluctuations of these opposite processes compensate each other closely.

Reporting summary

Further information on research design is available in the Nature Research Reporting Summary linked to this paper.

Data availability

The palaeobiological genus occurrence data are freely available for download in the Paleobiology Database https://paleobiodb.org/data1.2/occs/list.csv?datainfo&rowcount&base_name=Animalia&taxon_reso=genus&pres=regular&interval=cambrian,quaternary&envtype=marine. Other data—palaeotemperatures, tectonic rates and sea levels are available as supplementary data in the original cited articles.

Code availability

Macroevolutionary metrics were calculated in R v.3.6.0 using functions available in divDyn package. The scripts needed for the Phanerozoic-scale analysis of marine diversity with divDyn can be found at https://github.com/divDyn/ddPhanero/. Haar fluctuation, scaling and cross-Haar analyses were done using Mathematica custom-made code and can be accessed at http://www.physics.mcgill.ca/~gang/software/index.html.

51. Cornette, J. L., Lieberman, B. S. & Goldstein, R. H. Documenting a significant relationship between macroevolutionary origination rates and Phanerozoic pCO_2 levels. *Proc. Natl Acad. Sci. USA* **99**, 7832–7835 (2002).
52. Hannisdal, B. & Peters, S. E. Phanerozoic Earth system evolution and marine biodiversity. *Science* **334**, 1121–1124 (2011).
53. Mayhew, P. J., Bell, M. A., Benton, T. G. & McGowan, A. J. Biodiversity tracks temperature over time. *Proc. Natl Acad. Sci. USA* **109**, 15141–15145 (2012).
54. Mathes, G. H., van Dijk, J., Kiessling, W. & Steinbauer, M. J. Extinction risk controlled by interaction of long-term and short-term climate change. *Nat. Ecol. Evol.* **5**, 304–310 (2021).
55. Mathes, G. H., Kiessling, W. & Steinbauer, M. J. Deep-time climate legacies affect origination rates of marine genera. *Proc. Natl Acad. Sci. USA* **118**, e2105769118 (2021).
56. Roberts, G. G. & Mannion, P. D. Timing and periodicity of Phanerozoic marine biodiversity and environmental change. *Sci. Rep.* **9**, 6116 (2019).
57. Žliobaitė, I. & Fortelius, M. On calibrating the completometer for the mammalian fossil record. *Paleobiology* **48**, 1–11 (2021).
58. Valentine, J. W. & Walker, T. D. Diversity trends within a model taxonomic hierarchy. *Physica D* **22**, 31–42 (1986).
59. Sepkoski, J. J. & Kendrick, D. C. Numerical experiments with model monophyletic and paraphyletic taxa. *Paleobiology* **19**, 168–184 (1993).
60. Crampton, J. S., Cooper, R. A., Foote, M. & Sadler, P. M. Ephemeral species in the fossil record? Synchronous coupling of macroevolutionary dynamics in mid-Paleozoic zooplankton. *Paleobiology* **46**, 123–135 (2020).
61. Sepkoski, J. J. Ten years in the library: new data confirm paleontological patterns. *Paleobiology* **19**, 43–51 (1993).
62. Alroy, J. Successive approximations of diversity curves: ten more years in the library. *Geology* **28**, 1023–1026 (2000).
63. R Core Team. *R: A Language and Environment for Statistical Computing* (R Foundation for Statistical Computing, 2015).
64. Kocsis, A. T., Reddin, C. J., Alroy, J. & Kiessling, W. The R package divDyn for quantifying diversity dynamics using fossil sampling data. *Methods Ecol. Evol.* **10**, 735–743 (2019).
65. Kocsis, A. T., Alroy, J., Reddin, C. J. & Kiessling, W. Phanerozoic-scale global marine biodiversity analysis with the R package divDyn v0.7. divDyn vignette (2019).
66. Na, L. & Kiessling, W. Diversity partitioning during the Cambrian radiation. *Proc. Natl Acad. Sci. USA* **112**, 4702–4706 (2015).
67. Fan, J.-x et al. A high-resolution summary of Cambrian to Early Triassic marine invertebrate biodiversity. *Science* **367**, 272–277 (2020).
68. Raup, D. M. Cohort analysis of generic survivorship. *Paleobiology* **4**, 1–15 (1978).
69. Raup, D. M. Mathematical models of cladogenesis. *Paleobiology* **11**, 42–52 (1985).
70. Foote, M. Pulsed origination and extinction in the marine realm. *Paleobiology* **40**, 6–20 (2005).
71. Payne, J. L. & Heim, N. A. Body size, sampling completeness, and extinction risk in the marine fossil record. *Paleobiology* **46**, 23–40 (2020).
72. Hearing, T. W. et al. An early Cambrian greenhouse climate. *Sci. Adv.* **4**, eaar5690 (2018).
73. Goldberg, S. L., Present, T. M., Finnegan, S. & Bergmann, K. D. A high-resolution record of early Paleozoic climate. *Proc. Natl Acad. Sci. USA* **118**, e2013083118 (2021).
74. Schrag, D. P., DePaolo, D. J. & Richter, F. M. Reconstructing past sea surface temperatures: correcting for diagenesis of bulk marine carbonate. *Geochim. Cosmochim. Acta* **59**, 2265–2278 (1995).

75. Miller, K. G. et al. The Phanerozoic record of global sea-level change. *Science* **310**, 1293–1298 (2005).
76. Van der Meer, D. et al. Reconstructing first-order changes in sea level during the Phanerozoic and Neoproterozoic using strontium isotopes. *Gondwana Res.* **44**, 22–34 (2017).
77. Müller, R. D. & Dutkiewicz, A. Oceanic crustal carbon cycle drives 26-million-year atmospheric carbon dioxide periodicities. *Sci. Adv.* **4**, eaaq0500 (2018).
78. Kiessling, W. Long-term relationships between ecological stability and biodiversity in Phanerozoic reefs. *Nature* **433**, 410–413 (2005).
79. McKinney, M. L. & Oyen, C. W. Causation and nonrandomness in biological and geological time series: temperature as a proximal control of extinction and diversity. *Palaios* **4**, 3–15 (1989).
80. Haar, A. Zur theorie der orthogonalen funktionensysteme. *Math. Ann.* **69**, 331–371 (1910).

Acknowledgements We thank A. Kocsis for help with divDyn package functions. We also thank many contributors to the Paleobiology Database and the authors of descriptive taxonomic papers and geochemical analyses that generated the primary data used in this study. This research was supported by project S-MIP-21-9 'The role of spatial structuring in major transitions in macroevolution'. S.L. acknowledges the National Science and Engineering Council for some support. This paper is Paleobiology Database official publication 426.

Author contributions A.S. and S.L. developed the design of the study, analysed the data and wrote the text.

Competing interests The authors declare no competing interests.

Additional information
Supplementary information The online version contains supplementary material available at https://doi.org/10.1038/s41586-022-04867-y.
Correspondence and requests for materials should be addressed to Andrej Spiridonov or Shaun Lovejoy.
Peer review information *Nature* thanks Jurgen Kurths, Gene Hunt, Appy Sluijs and the other, anonymous, reviewer(s) for their contribution to the peer review of this work. Peer reviewer reports are available.

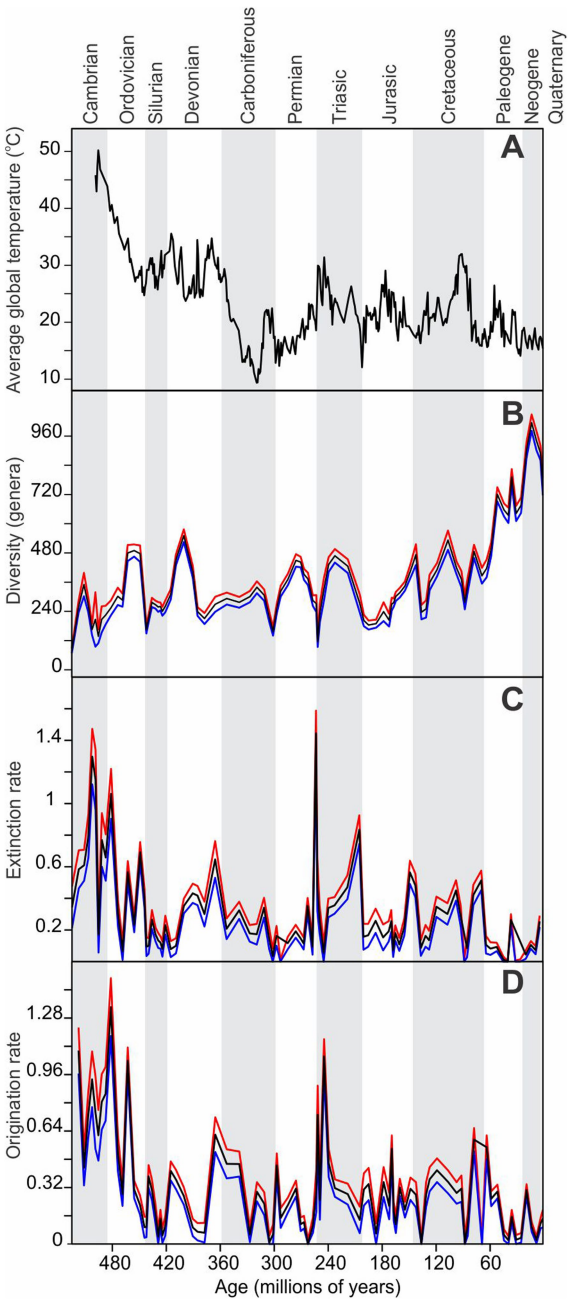

Extended Data Fig. 1 | Macroevolutionary and paleoclimate time series. **A**. Average global surface water temperatures (*T*) Song and others (2019) data[28], **B** marine animal genus diversity (*D*), **C** second-for-third genus extinction rates per bin (*E*), **D** second-for-third origination rates per bin (*O*). Paleobiological patterns are per bin averages with $\pm\sigma$ confidence intervals based on 100 bootstrap replications.

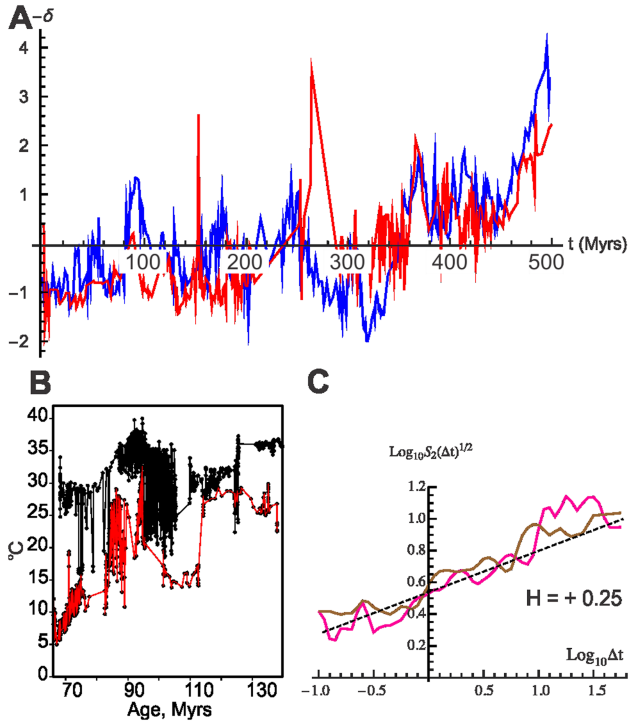

Extended Data Fig. 2 | Paleoclimate time series and time scaling. A. Song et al., 2019 (blue) and Veizer et al., 1999 (red) global sea water paleotemperature stacks[32,33] expressed in $\delta^{18}O$ ‰ units as a function of age (time flows from right to left). The Song et al., 2019 data was standardized by setting mean to zero and standard deviations were made equal. **B** Cretaceous sea surface water temperatures based on TEX_{86} and $\delta^{18}O_{pl}$ data[73] for low latitudes (black) [n = 2856 temperature estimates] and high latitudes (red)[n = 638 temperature estimates] in °C. **C**. Haar fluctuation scaling curves for high latitude (pink), and low latitude (brown) Cretaceous sea surface temperatures (in °C); timescales shown in $\log_{10}$ Myr; dashed line shows scaling pattern with H = +0.25.

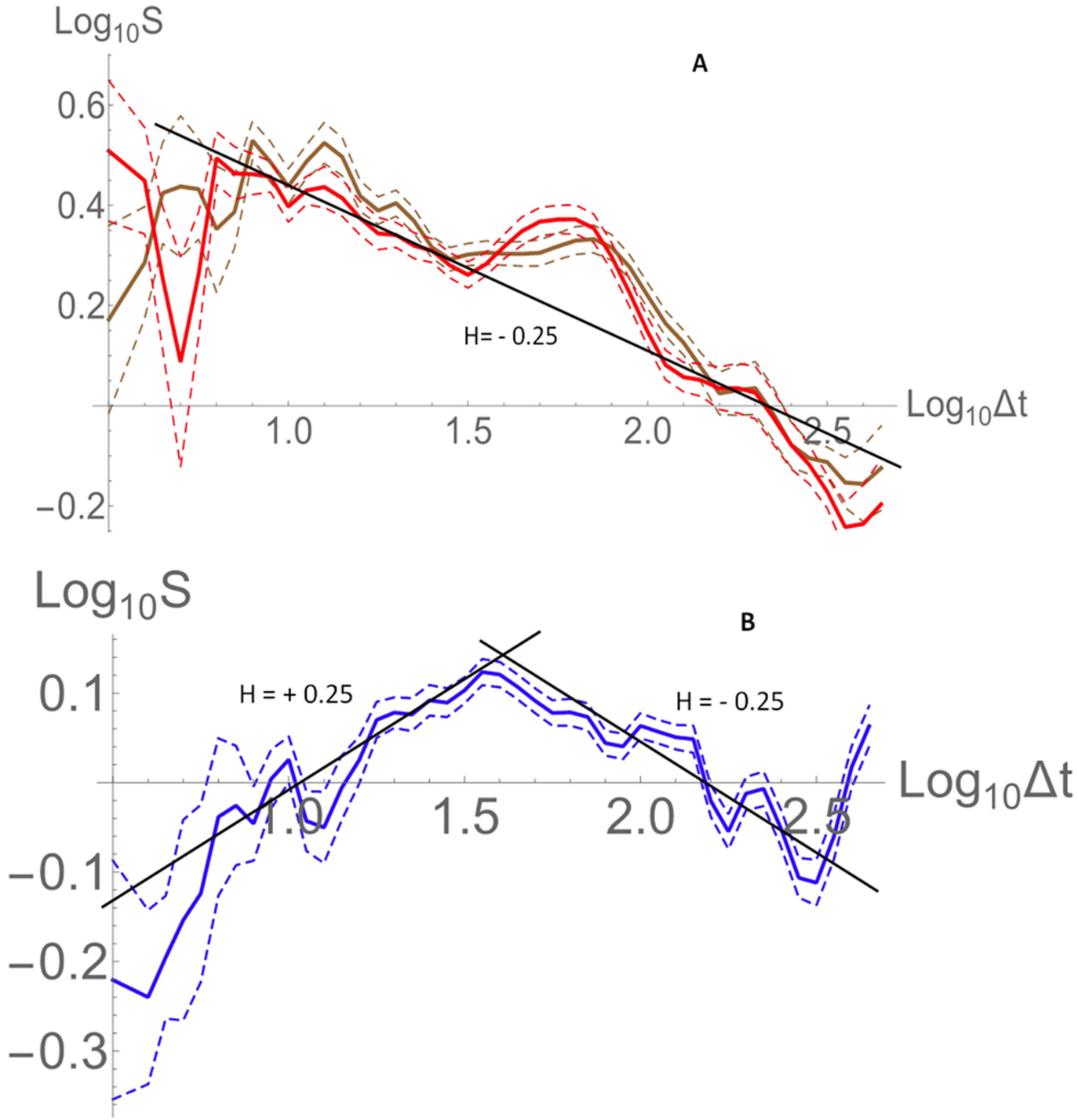

Extended Data Fig. 3 | Scaling of macroevolutionary time series with confidence bands. Haar fluctuation scaling curves with standard errors based on the analysis of 100 subsamplings: **A** origination (red) and extinction (brown) rates (x10)[as in the Fig. 1]; **B** genus diversity (x0.01))[as in the Fig. 1]. Timescales shown in $\log_{10}$ Myr.

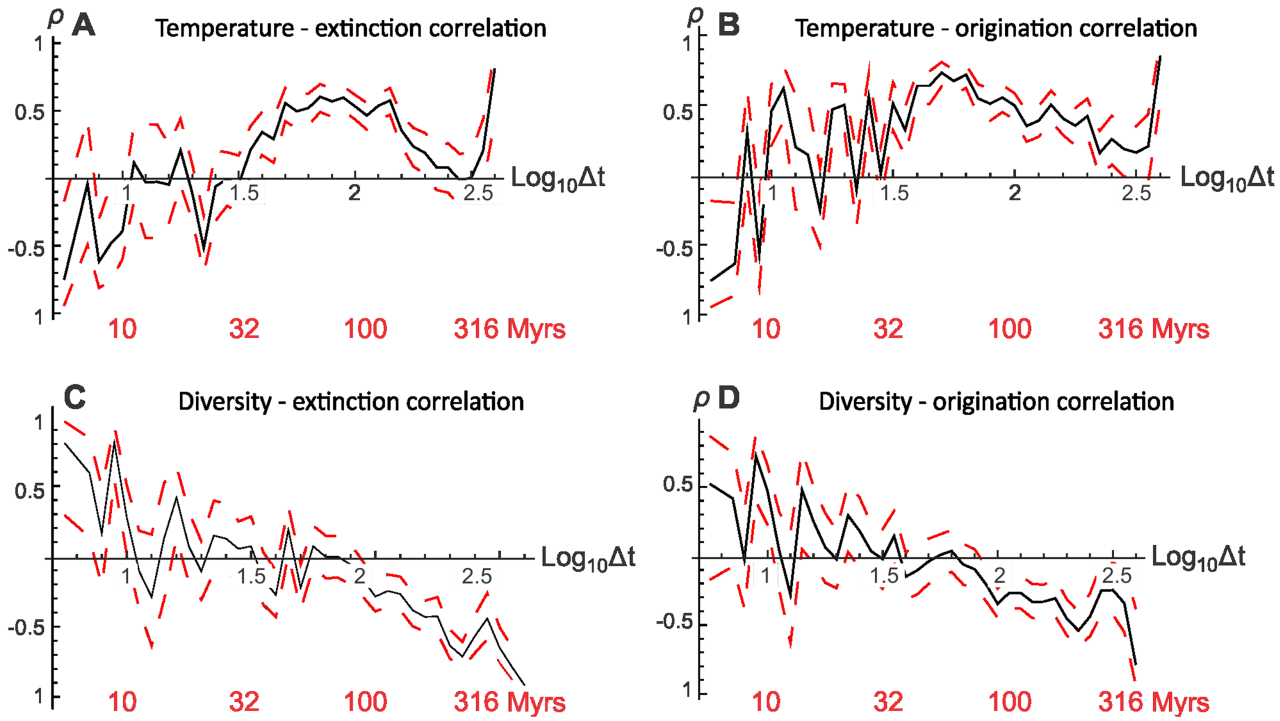

Extended Data Fig. 4 | Time-dependant correlations. scale-dependant correlations of fluctuations in **A** extinction rates with temperatures, time in *Myr*. Same for **B** origination rates with temperatures; **C** global diversity levels with extinction rates; **D** global diversity levels with origination rates. Mean (black) and one standard deviation confidence limits dashed red. Mean (black) and one standard deviation confidence limits dashed red (16–84%).

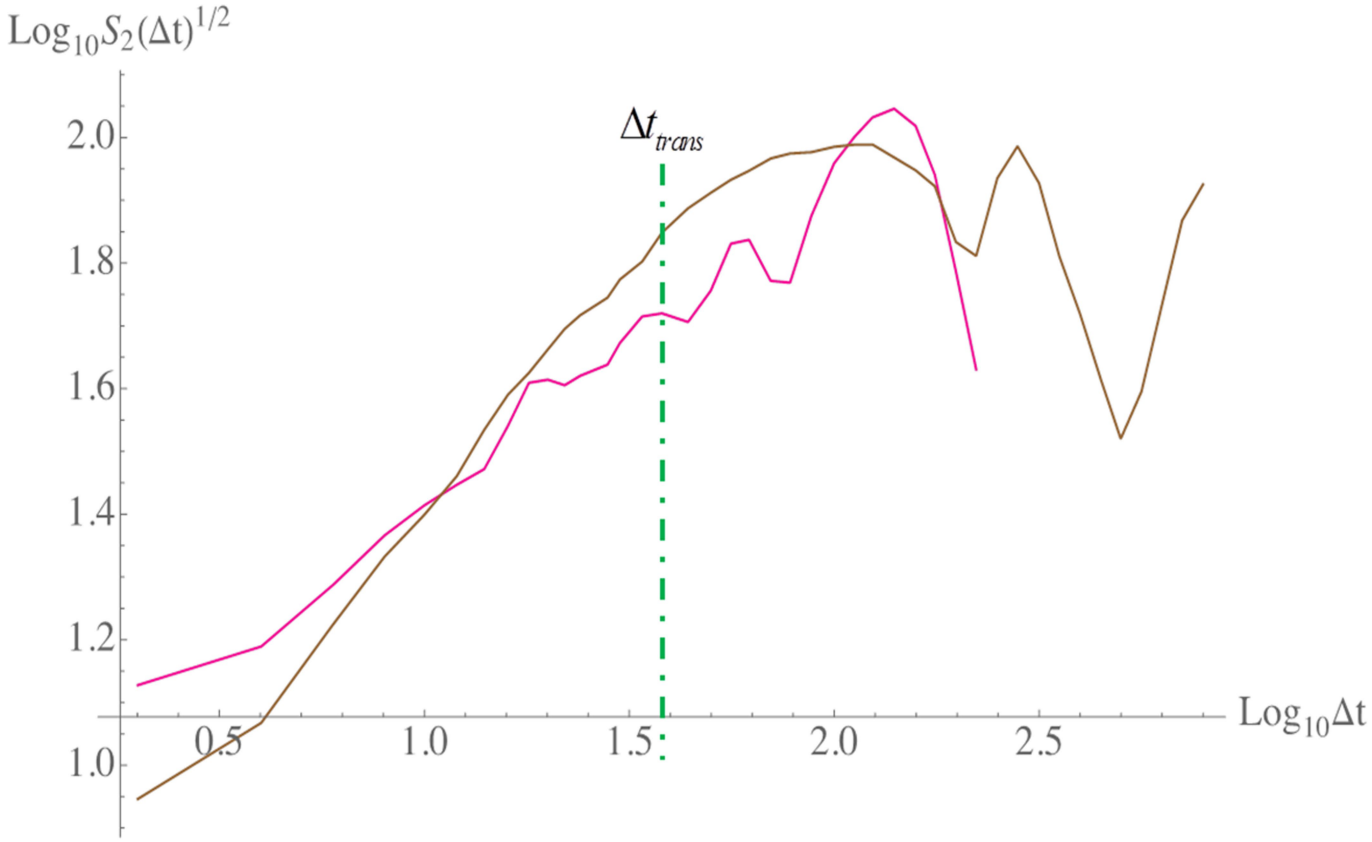

Extended Data Fig. 5 | Time scaling of the global sea level and sea floor spreading. Haar fluctuation scaling of the sea level[75] (in m from the present level) during the Phanerozoic and Neoproterozoic (brown), and of the sea floor production rates[76] through the Meso-Cenozoic (m^2/year /3 x 10^4) (pink). Timescales shown in $\log_{10}$ Myr. Both geophyscal variables scale positively at least to the timescale of 100 Myr. Δt_{trans} signifies critical transition time from the positive to the negative diversity scaling, and the start of synchronization of macroevolutionary rates. Sea level and tectonic activity scales positively well beyound this critical threshold.

nature portfolio

Corresponding author(s): Andrej Spiridonov

Last updated by author(s): Apr 15, 2022

Reporting Summary

Nature Portfolio wishes to improve the reproducibility of the work that we publish. This form provides structure for consistency and transparency in reporting. For further information on Nature Portfolio policies, see our Editorial Policies and the Editorial Policy Checklist.

Statistics

For all statistical analyses, confirm that the following items are present in the figure legend, table legend, main text, or Methods section.

n/a	Confirmed
☐	☒ The exact sample size (*n*) for each experimental group/condition, given as a discrete number and unit of measurement
☐	☒ A statement on whether measurements were taken from distinct samples or whether the same sample was measured repeatedly
☒	☐ The statistical test(s) used AND whether they are one- or two-sided *Only common tests should be described solely by name; describe more complex techniques in the Methods section.*
☐	☒ A description of all covariates tested
☐	☒ A description of any assumptions or corrections, such as tests of normality and adjustment for multiple comparisons
☐	☒ A full description of the statistical parameters including central tendency (e.g. means) or other basic estimates (e.g. regression coefficient) AND variation (e.g. standard deviation) or associated estimates of uncertainty (e.g. confidence intervals)
☒	☐ For null hypothesis testing, the test statistic (e.g. *F*, *t*, *r*) with confidence intervals, effect sizes, degrees of freedom and *P* value noted *Give P values as exact values whenever suitable.*
☒	☐ For Bayesian analysis, information on the choice of priors and Markov chain Monte Carlo settings
☒	☐ For hierarchical and complex designs, identification of the appropriate level for tests and full reporting of outcomes
☐	☒ Estimates of effect sizes (e.g. Cohen's *d*, Pearson's *r*), indicating how they were calculated

Our web collection on statistics for biologists contains articles on many of the points above.

Software and code

Policy information about availability of computer code

Data collection	No software assisted data collection was done
Data analysis	Macroevolutionary metrics were calculated in the R computational environment (R version 3.6.0) using functions available in 'divDyn' package. The scripts needed for the Phanerozoic scale analysis of marine diversity with the 'divDyn' package could be found in package developers' Adam Kocsis' site https://github.com/divDyn/ddPhanero/ . Haar fluctuation, scaling, and cross-Haar analyses were done using Mathematica custom made code and could be freely accessed at http://www.physics.mcgill.ca/~gang/software/index.html ."

For manuscripts utilizing custom algorithms or software that are central to the research but not yet described in published literature, software must be made available to editors and reviewers. We strongly encourage code deposition in a community repository (e.g. GitHub). See the Nature Portfolio guidelines for submitting code & software for further information.

Data

Policy information about availability of data

All manuscripts must include a data availability statement. This statement should provide the following information, where applicable:

- Accession codes, unique identifiers, or web links for publicly available datasets
- A description of any restrictions on data availability
- For clinical datasets or third party data, please ensure that the statement adheres to our policy

The paleobiological genus occurrence data are freely available for download in the Paleobiology Database https://paleobiodb.org . Other data - paleotemperatures, tectonic rates, and sea levels are available as supplementary data in the original cited articles. Additional figures are presented as Extended Data Figs. 1–5.

Field-specific reporting

Please select the one below that is the best fit for your research. If you are not sure, read the appropriate sections before making your selection.

☐ Life sciences ☐ Behavioural & social sciences ☒ Ecological, evolutionary & environmental sciences

For a reference copy of the document with all sections, see nature.com/documents/nr-reporting-summary-flat.pdf

Ecological, evolutionary & environmental sciences study design

All studies must disclose on these points even when the disclosure is negative.

Study description	This study reveals Haar fluctuation scaling behaviour of genus level marine animal diversity, originations, and extinctions, as well as marine paleotemperatures through the Phanerozoic. The scale-by-scale correlations between Haar fluctuations reveal details of interactions and qualitative changes in the forcing of global scale macroevolutionary processes. Genus level marine Animalia occurrence data downloaded from the Paleobiology Database. Paleoclimate data acquired from the Weizer et al., 1999, and Song et al., 2019 articles.Tectonic proxies from Muller and Dutkiewicz, 2018; Sea level data from van der Meer et al., 2017, Cretaceous sea-surface temperature data from O'Brien et al., 2017.
Research sample	All available fossil marine animals (phylogenetically defined Animalia) from the marine Phanerozoic fossil record of the Paleobiology Database were researched. 765,125 of unique space/time/genus occurrence records of marine fossil animals from the Paleobiology Database were downloaded and further used in calculation of macroevolutionary metrics. As proxies for global environmental geophysical states 388 global temperature estimates were used in the cross scale correlations and other analyses from the Song. et al., 2019; 231 crustal production estimates from Muller and Dutkiewicz, 2018; and 837 sea level estimates from van der Meer et al., 2017. 2856 low latitude sea-surface temperature estimates, and 639 high latitude sea surface temperature estimates from O'Brien et al., 2017.
Sampling strategy	All regular (non-ichnofossil) animal genus level taxa and their occurrences were recorded in the bound of the Phanerozoic. The data are of global scope in each time bin. Occurrences were assigned to the Paleobiology Database operational stage resolution. In order to sample standardize the available taxonomic information SQS subsampling was applied in 'divDyn' R package, with a value of shareholder quorum equal to q=0.7.
Data collection	Genus occurrence data was downloaded on June 5th 2019 by A.S. from the https://paleobiodb.org/data1.2/occs/list.csv?datainfo&rowcount&base_name=Animalia&taxon_reso=genus&pres=regular&interval=cambrian,quaternary&envtype=marine in the *.csv format. The data constitutes taxonomic identifiers, fossil preservation environments and time ranges of genus occurrences of animal taxa, which were collected from tens of thousands of published scientific articles, and monographs by contributors of the Paleobiology Database.
Timing and spatial scale	The temporal scale of taxonomic data spans the whole Phanerozoic eon (541-0 Myrs BP). Its spatial scale is global. The macroevolutionary variables were assigned to central points of Paleobiology Database stage level bins (525 Myrs - the start; 1.3 the end). The durations of bins are variable and stratigraphically determined. The average duration of a bin is 5.9 Myrs.
Data exclusions	No data was excluded.
Reproducibility	The genus occurrence data can be freely downloaded from the Paleobiology Database. The macroevolutionary time series could be generated using standard divDyn scripts. Cross scale analyses could repeated using custom made Mathematica code available from S. L. website.
Randomization	The calculation of macroevolutionary metrics was done by averaging 100 SQS subsamples of the total data set in order to reveal the internal variability.
Blinding	This is not relevant in this study. No living subjects were investigated in this study.

Did the study involve field work? ☐ Yes ☒ No

Reporting for specific materials, systems and methods

We require information from authors about some types of materials, experimental systems and methods used in many studies. Here, indicate whether each material, system or method listed is relevant to your study. If you are not sure if a list item applies to your research, read the appropriate section before selecting a response.

Materials & experimental systems

n/a	Involved in the study
☒	☐ Antibodies
☒	☐ Eukaryotic cell lines
☐	☒ Palaeontology and archaeology
☒	☐ Animals and other organisms
☒	☐ Human research participants
☒	☐ Clinical data
☒	☐ Dual use research of concern

Methods

n/a	Involved in the study
☒	☐ ChIP-seq
☒	☐ Flow cytometry
☒	☐ MRI-based neuroimaging

Palaeontology and Archaeology

Specimen provenance: This is irrelevant to this study. Information from publicly available database was used.

Specimen deposition: This is irrelevant to this study. No physical specimens were researched in this study.

Dating methods: No new dates were generated in this study.

☐ Tick this box to confirm that the raw and calibrated dates are available in the paper or in Supplementary Information.

Ethics oversight: *Identify the organization(s) that approved or provided guidance on the study protocol, OR state that no ethical approval or guidance was required and explain why not.*

Note that full information on the approval of the study protocol must also be provided in the manuscript.